

Inhibitory effects of recombinant human endostatin combined with cisplatin on transplanted human gastric carcinoma in nude mice.

Dinuo Li^{1,2}, Hongzhi Sun^{1,2*}, Yubin Wang^{1,3}, Qiang Li^{1,3}, Lei Wang⁴

¹Department of General Surgery, the First Affiliated Hospital of Jinzhou Medical University, Jinzhou, PR China

²Department of General Surgery, School of Medicine, Shandong University, Jinan, PR China

³Department of General Surgery, Xi'an Jiaotong University Health Science Center, Xi'an, PR China

⁴Department of Cardiology, the First Affiliated Hospital of Jinzhou Medical University, Jinzhou, PR China

Abstract

The aim of this study was to observe the impact of recombinant human endostatin (Endostar) combined with cisplatin (En+Ci) on gastric carcinoma xenografts in nude mice. The nude mice model with gastric carcinoma xenografts was randomly divided into the control group, 0.5 mg/kg En group, 5 mg/kg Ci group, and 5 mg/kg En+5 mg/kg Ci group for the treatment; Microvessel Density (MVD) was performed to detect the expression of CD34, mRNA and protein detection was performed to detect the expression changes of inhibitor of DNA binding 1 (ID1) and Vascular Endothelial Growth Factor (VEGF), and transmission electron microscopy was performed to detect the apoptosis. Compared with the control group, the expressions of ID1, VEGF, and MVD in group En were decreased, the tumor size in group Ci was decreased, and the tumor size in group En+Ci was decreased significantly together with significant apoptosis; the MVD expressions in group En and En+Ci were 11.38 ± 1.25 and 10.93 ± 1.54 , respectively, showing no significance ($P > 0.05$). En can inhibit the angiogenesis by reducing the expression of ID1, and promote the apoptosis of tumor cells, thus co-achieving the results of inhibiting the growth and metastasis of tumor, and this can provide a new way of thinking for neoadjuvant chemotherapies of gastric carcinoma.

Keywords: Endostar, Cisplatin, ID1, Gastric carcinoma.

Accepted on October 17, 2017

Introduction

Gastric Carcinoma (GC) is vessel-rich solid tumor, which is one of the most common malignancies in China. Its mortality still lies in the first place among malignant tumors. Because of its occult onset, it often cannot be detected and diagnosed early, leading to its high mortality. Surgical resection is currently the only possible cure for GC, but its clinical five-year survival rate for advanced GC patients is still hovering around 50%, and patients' postoperative quality of life is significantly decreased [1,2]. Early metastasis of cancer cells is the leading cause of poor prognosis in advanced GC cases, but the current understanding of the molecular mechanisms of GC metastasis is still very limited. As one anti-angiogenic drug produced in China, Endostar (recombinant human endostatin) has an inhibitory effect on tumor angiogenesis [3], has been widely used as one targeted assistance therapy toward various tumors recently [4], and has exhibited such advantages as reliable multi-target efficacies, small side effects, and sensitizing other cell killing drugs [5]. Cisplatin is a cytotoxic drug widely recognized in the treatment of malignant tumors [6-10]. In this study, these two drugs were combined and

applied against nude mice with GC xenografts, hoping to observe and compare their impact on the tumor markers, apoptosis, and angiogenesis with other treatment methods, thus providing theoretical basis for clinical applications as well as providing new ideas for preventing and controlling the invasion and metastasis of GC.

Materials and Methods

Preparation of nude mice model

The Human GC SGC-7901 cells (Cell Bank of Chinese Academy of Sciences, China) were cultured in RPMI1640 medium (Gibco, USA) containing 10% FBS at 37°C and in 5% CO₂. When the cells grew to 80% of the flask area, 0.25% trypsin was used for 1 min digestion at 37°C; after discarded the trypsin, fresh medium was added and pipetted the residual into single cell suspension, followed by sub-packaging and passage. The 3rd generation SGC-7901 cell suspension was then implanted subcutaneously into the axillary subcutaneous tissue of 32 nude mice (Experimental Animal Center of Dalian Medical University, China). This study was carried out in strict

accordance with the recommendations in the Guide for the Care and Use of Laboratory Animals of the National Institutes of Health. The animal use protocol has been reviewed and approved by the Institutional Animal Care and Use Committee (IACUC) of Shandong University.

Grouping

The Balb/c tumor-bearing nude mice were randomly divided into four groups (n=8), and intervened with En (Pioneer Pharmaceutical Co., Ltd., Yantai, Shandong, China) and Ci (Jinzhou Jiutai Pharmaceutical) when the tumor diameter grew to 0.8 cm; the control group was not intervened, while other experimental groups were applied 5 mg/kg Ci, 0.5 mg/kg En, and 5 mg/kg Ci combined with 5 mg/kg En, respectively. En was subcutaneously administrated around the tumor once every other day, and Ci was intraperitoneally applied once every other 3 d; the whole course was 4 w, during which period the daily activities, feeding, and drinking water changes of the nude mice were recorded, and the body weight of the nude mice was measured weekly using one electronic balance.

Sampling

After 4 w treatment, the experimental groups were withdrawn 1 w for the residual effects of blood drug, and then the mice were killed with chloral hydrate so as to sample the tumor tissue for related measurement of the tumor.

Immunohistochemistry

The paraffin-embedded tumor tissue was performed slicing, dewaxing, and antigen repair. The primary antibody rabbit anti-human CD34 (Beijing ZSGB-Bio Origene Co., Ltd, China) was diluted 1: 50 with Phosphate Buffered Saline (PBS), and PBS was used to replace the primary antibody as a negative control. The secondary antibody goat anti-rabbit IgG-HRP was diluted (1:200). The slices were performed DAB coloration, mounting, and observation. The positive standard of CD34 protein expressed by GC cells was the brown particles appearing in the cytoplasm and on the cell membrane; the Microvessel Density (MVD) was counted using the Weidner microvessel counting method.

Reverse transcription polymerase chain reaction (RT-PCR)

The fresh frozen tissue samples of each group were performed total RNA extraction and RT-PCR amplification according to the instructions of RT-PCR kit (TaKaRa, Japan). The cycle parameters were: pre-denaturation at 95°C for 10 min, denaturation at 94°C for 1 min, annealing at 60°C for 1 min, and extension at 72°C for 2 min, and after 30 cycles, extension at 72°C for 8 min. The PCR products were separated by agarose gel electrophoresis and observed by one ultraviolet analyzer. The average gray values of the positive electrophoresis bands were determined by the Lab Works software, and the ratio of average gray values of the target gene and β -actin bands was calculated as the relative expression.

Primer sequences: ID1: positive-sense strand 5'-CAAGTGGCCAGAGGCATGCACTT-3'; antisense strand: 5'-GATGTAGTC TTTACCATCCTGTTG-3'; Vascular Endothelial Growth Factor (VEGF): positive-sense strand 5'-GAAGTGGTGAAGTTCATGGATGTC-3'; antisense strand 5'-CGATCGTTCTGTATCACTCTTTCC-3' (TaKaRa, Inc., Japan).

Western blot

The fresh frozen tissue samples of each group were washed 3 times with pre-cooling PBS, and then added 400 μ l of lysis solution for 30 min on-ice lysis; after centrifuged at 4°C, 14000 rpm \times 5 min, the supernatant was detected the protein concentration and performed sodium dodecyl sulfate polyacrylamide gel electrophoresis (SDS-PAGE). After transferred onto films, the films were closed using TBST containing 5% albumin from bovine serum (BSA) at room temperature for 1 h, followed by adding the antibodies of ID1, VEGF, and β -actin (1:500) (Santa Cruz, USA) for overnight incubation at 4°C; after added the secondary antibodies (1:1), the films were washed and developed.

Transmission electron microscope (TEM)

The samples were fixed with 4% glutaraldehyde, washed three times with 0.1 mol/L PBS (15 min each time), and then fixed with osmium for 2 h. After dehydrated with gradient acetone (30%, 50%, 70%, 80%, 90%, and 100%, respectively, 20 min each gradient except for 100% (2 \times 30 min)), the samples were soaked into the mixture of embedding agent and acetone (1:1) at 37°C for 1 h, followed by overnight soaking into the mixture of embedding agent and acetone (3:1) at 37°C. After soaked into pure embedding agent at 37°C for 24 h, the samples were performed polymerization at 60°C for 48 h. One Leica UCT ultramicrotome was used to prepare the slices, followed by observing the apoptosis using one Hitachi H-7500 transmission electron microscope.

Statistical analysis

SPSS20.0 for windows was used for the statistical analysis; the measurement data were expressed as mean \pm standard deviation ($\bar{x} \pm s$); the intergroup comparison used the t-test, and multi-group comparison used the single-factor analysis of variance; the count data were compared using the χ^2 test and the exact probability of four fold table method, with $P < 0.05$ considered as statistical significance.

Results

General information

The nude mice exhibited good diet, drinking, and activities before xenografting, and the four groups showed no difference in the body weight. The activities of the nude mice in group Ci were significantly decreased after medication, together with dietary intake and body weight decreasing, which lasted until the experiment ended. The body weight of the nude mice in the

Inhibitory effects of recombinant human endostatin combined with cisplatin on transplanted human gastric carcinoma in nude mice

control group, En, En+Ci kept growing until the experiment ended (Table 1). At the end of the experiment, the average body weights of the nude mice in group En+Ci, En, Ci and control were 19.75 ± 0.33 g, 22.50 ± 0.59 g, 14.21 ± 0.83 g, and 21.98 ± 0.91 g, respectively, exhibiting significant differences among the four groups ($P < 0.05$). The body weight of nude mice in group Ci was significantly lower than the other groups ($P < 0.05$), while those between the control group and group En showed no significance ($P = 0.53$). However, there was significant differences in the body weight between group En+Ci and the control group or group En ($P < 0.05$).

Tumor volume changes

The volumes of subcutaneous transplanted tumors in the nude mice of the four groups gradually increased with the experiment going. The control group exhibited rapid increase, while the other three groups exhibited slow increase. When the experiment ended, the mean volumes in group En+Ci, En, Ci, and the control were (0.29 ± 0.13 cm³), (0.52 ± 0.29 cm³), (0.60 ± 0.31 cm³), and (1.29 ± 0.65 cm³), respectively, showing statistically significant differences among the groups ($P = 0.032 < 0.05$) (Table 2). There were significant differences between the control group and group Ci, EN, or En+Ci ($P < 0.05$), while the pairwise comparison among group Ci, EN, and En+Ci showed no significant difference ($P > 0.05$). The experimental results showed that En can inhibit tumor growth in the nude mice, but it has no tumor elimination effect (namely promoting the necrosis of tumor so as to shrink the tumor).

Quality changes of tumor

At the end of the experiment, the average weights of the tumor mass in group En+Ci, En, Ci, and the control were 0.43 ± 0.25 g, 0.84 ± 0.33 g, 0.79 ± 0.26 g, and 1.81 ± 0.75 g, respectively, exhibiting significant differences among the four groups (Table 2) ($P = 0.015 < 0.05$). There were significant differences between the control group and group Ci, EN, or En+Ci ($P < 0.05$), but there was no significant difference in the pairwise comparison among group En+Ci, En, Ci ($P > 0.05$).

Immunohistochemistry

The results showed that the MVD differences among the groups were statistically significant ($P = 0.000$) (Figure 1), among which group En and En+Ci exhibited more obvious t inhibitory effects against tumor angiogenesis, the MVD values of which were 11.38 ± 1.25 and 10.93 ± 1.54 , showing no significant difference ($P > 0.05$). The difference in MVD between group CI and the control group was also statistically significant (16.17 ± 1.33 and 23.73 ± 2.40 , $P < 0.05$).

RT-PCR

The RT-PCR results showed that the ID1 and VEGF mRNAs in group En and En+Ci were statistically downregulated than the control group, with the relative OD values of ID1 in group EN and En+Ci as 0.326 ± 0.083 and 0.015 ± 0.002 , and those

of VEGF in group EN and En+Ci as 0.257 ± 0.049 and 0.031 ± 0.006 ($P > 0.05$). There was no significant difference in the mRNA expression of ID1 and VEGF between group Ci and the control ($P > 0.05$) (Figure 2).

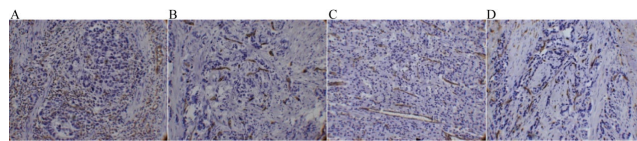


Figure 1. The CD34 protein is the highly expressed brown particle in the cytoplasm. A: 0 mg/kg; B: group EN; C: group Ci; D: group En+Ci.

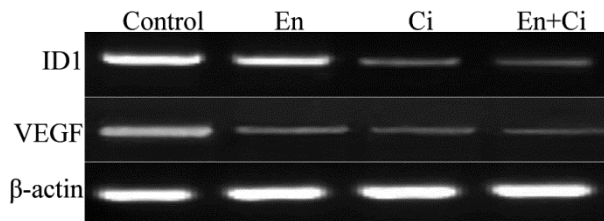


Figure 2. Detection of expressions of ID1 and VEGF mRNAs by RT-PCR.

Western blot

The results showed that ID1 and VEGF proteins in group En and En+Ci were statistically downregulated than the control group, with the relative OD values of ID1 in group EN and En+Ci as 0.279 ± 0.051 and 0.012 ± 0.003 , and those of VEGF in group EN and En+Ci as 0.236 ± 0.084 and 0.026 ± 0.009 ($P > 0.05$). There was no significant difference in the protein expression of ID1 and VEGF between group Ci and the control ($P > 0.05$) (Figure 3).

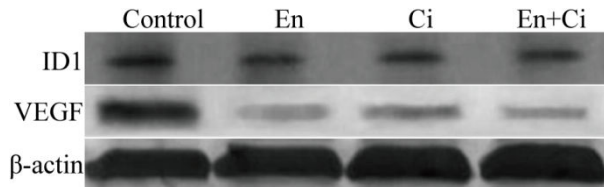


Figure 3. Detection of expressions of ID1 and VEGF proteins by Western blot.

Ultrastructural changes

TEM revealed that the tumor cells in the nude mice in group En and En+Ci exhibited apoptotic cells, which mainly manifested as nuclear fragments were visible, the rough endoplasmic reticulum mildly expanded together with the phenomenon of degranulation; the mitochondria exhibited myeloid-like changes (Figure 4A). No such apoptotic changes can be seen in the control group and group Ci, but a large number of degenerated and necrotic cells can be found with the main performance as most of the mitochondrial ridge disappeared, the mitochondrial membrane exhibited defects and myeloid-like changes, the cytoplasm exhibited edema, degeneration, and necrosis, and the rough endoplasmic reticulum exhibited high-degree expansion and the

phenomenon of degranulation (Figure 4B). The results showed that En can not only inhibit the tumor angiogenesis but also directly inhibit the proliferation of some tumor cells by promoting the apoptosis of tumor cells, thus achieving the inhibitory effects against the tumor.

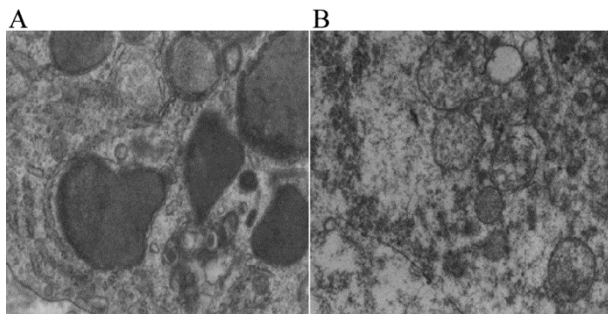


Figure 4. Observation of apoptosis by TEM.

Table 1. Body weights of nude mice of each group.

Group	Initial body weight (g)	Final body weight (g)
En+Ci	18.26 ± 0.35	19.75 ± 0.33
En	18.17 ± 0.73	22.50 ± 0.59
Ci	17.99 ± 0.41	14.21 ± 0.83 [*]
Control	18.62 ± 0.74	21.98 ± 0.91

Note: ^{*}P<0.05 compared with other three groups.

Table 2. Weights and volumes of tumor in nude mice of different groups.

Group	Tumor weight (g)	Tumor volume (cm ³)
En+Ci	0.43 ± 0.25	0.29 ± 0.13
En	0.84 ± 0.33	0.52 ± 0.29
Ci	0.79 ± 0.26	0.60 ± 0.31
Control	1.81 ± 0.75	1.29 ± 0.65 [*]

Note: ^{*}P<0.05 compared with other three groups.

Discussion

Endostar is a multi-target drug developed by China that can confront the angiogenesis of tumors. A large number of pre-clinical and clinical trials have confirmed its effectiveness and safety as a new targeted anti-tumor agent [11,12]. The advantages of Endostar also include: the targets directly expose in the blood, so it'll facilitate the direct role of Endostar; the target genes are expressed stably, so it's not easy to generate drug resistance; it doesn't need to consider tumor tissue's specificity; it can inhibit tumor metastasis, has downstream amplification effects while relatively less adverse reactions [13,14]. Endostar can exhibit synergistic effects when combined with radiotherapy and chemotherapy: 1) can normalize the angiogenesis in tumor regions, thus reducing interstitial hypertension and facilitating the delivery of chemotherapy drugs to tumor regions; 2) Anoxia in local tumor

regions caused by radiotherapy and chemotherapy can promote the expression of VEGF, thus helping tumor cells to resist the apoptotic mechanisms induced by radiotherapy and chemotherapy, while the combination of Endostar can prevent this secondary protective effects and sensitize the therapeutic responses.

Cisplatin is a cytotoxic drug with significant anti-tumor effects [15-19]. In this study, we collaborated Endostar and cisplatin so as to evaluate their treatment effects against GC xenografts in nude mice by observing the changes of tumor size, MVD, and expression changes of ID1 and VEGF. 1) Compared with the control group, all the experimental groups showed reduced tumor size, indicating that killing cell and inhibiting the angiogenesis can both inhibit the growth of GC xenografts in nude mice; however, there was no significant difference among the experimental groups (P>0.05). The reason of this result may be caused by short tumor cell incubation time, drug application time, and drug concentration. The body weight loss in group Ci was very obvious, so the nude mice exhibited significant ematiation, while the nude mice in group En and En+Ci gradually increased, indicating that Endostar can reduce chemotherapy-induced side effects such as weight loss, etc. 2)The immunohistochemical results of MVD showed that En+Ci exhibited significant inhibitory effects against MVD; group Ci also showed difference than the control group, but the inhibitory effects were significantly lower than those in group En and En+Ci, indicating that Endostar has significant inhibitory effects against vessels. 3) It has been confirmed that the inhibitory effects of endostar on MVD is realized by inhibiting the expression of the VEGF upstream factor ID1 [20]. The Western and RT-PCR results were consistent with the above-mentioned theory, but the effects of cisplatin on this factor are not significant, indicating that the action mechanism of Endostar is consistent with the previous results. 4) The results of TEM showed that the tumor cells treated with Endostar or En+Ci exhibited apoptosis, which was not obvious in the control group and group Ci, so we can further believe that endostar can not only inhibit the angiogenesis of tumors but also directly inhibit the proliferation of partial tumor cells through promoting the apoptosis of tumor cells, thus exhibiting its tumor inhibitory roles [21-25].

In conclusion, this study established the SGC7901 xenograft model in nude mice to observe the impact of Endostar on the growth of nude mice and tumor. It was found that Endostar can inhibit the angiogenesis and promote the apoptosis of tumor cells by decreasing the expression of ID1, thus achieving the effects of inhibiting the growth and metastasis of tumors, at the same time the repeat intrapleural injection of Endostar on nude mouse model of malignant pleural effusion also got very good outcome, so this study provides a new way of thinking for neoadjuvant chemotherapies of GC.

Acknowledgements

This work was funded by Liaoning Natural Science Foundation of China (item number: 20170540334).

Conflicts of Interest

The authors declare no conflict of interest.

References

1. Altan B, Yokobori T, Ide M, Bai T, Yanoma T, Kimura A, Kogure N, Suzuki M, Bao P, Mochiki E, Ogata K, Handa T, Kaira K, Nishiyama M, Asao T, Oyama T, Kuwano H. High expression of MRE11-RAD50-NBS1 is associated with poor prognosis and chemoresistance in gastric cancer. *Anticancer Res* 2016; 36: 5237-5247.
2. Dassen AE, Bernards N, Lemmens VE, van de Wouw YAJ, Bosscha K, Creemers GJ. Phase II study of docetaxel, cisplatin and capecitabine as preoperative chemotherapy in resectable gastric cancer. *World J Gastrointest Surg* 2016; 8: 706-712.
3. Haubold M1, Weise A, Stephan H, Dünker N. Bone morphogenetic protein 4 (BMP4) signaling in retinoblastoma cells. *Int J Biol Sci* 2010; 6: 700-715.
4. Rothschild SI1, Kappeler A, Ratschiller D, Betticher DC, Tschan MP. The stem cell gene inhibitor of differentiation 1 (ID1) is frequently expressed in non-small cell lung cancer. *Lung Cancer* 2011; 71: 306-311.
5. Franco TH, Khan A, Joshi V, Thomas B. Takotsubo cardiomyopathy in two men receiving bevacizumab for metastatic cancer. *Ther Clin Risk Manag* 2008; 4: 1367-1370.
6. Wu B, Chen H, Shen J, Ye M. Cost-effectiveness of adding rh-endostatin to first-line chemotherapy in patients with advanced non-small-cell lung cancer in China. *Clin Ther* 2011; 33: 1446-1455.
7. Shrestha S, Song YW, Kim H, Lee DS, Cho SK. Sageone, a diterpene from *Rosmarinus officinalis*, synergizes with cisplatin cytotoxicity in SNU-1 human gastric cancer cells. *Phytomedicine* 2016; 23: 1671-1679.
8. Goody RB, MacKay H, Pitcher B, Oza A, Siu LL, Kim J, Wong RK, Chen E, Swallow C, Knox J, Kassam Z, Cummings B, Feld R, Hedley D, Liu G, Krzyzanowska MK, Dinniwell R, Brade AM, Dawson LA, Pintilie M, Ringash J. Phase 1/2 study of the addition of cisplatin to adjuvant chemotherapy with image guided high-precision radiation therapy for completely resected gastric cancer. *Int J Radiat Oncol Biol Phys* 2016; 96: 994-1002.
9. Carmona-Bayonas A, Jimenez-Fonseca P, Lorenzo ML, Ramchandani A, Martinez EA. On the effect of triplet or doublet chemotherapy in advanced gastric cancer: results from a national cancer registry. *J Natl Compr Canc Netw* 2016; 14: 1379-1388.
10. Hosseinzadeh A, Somi MH, Dolatkhah H, Esfahani A, Kafil HS. The effect of ω -fatty acids on mRNA expression level of PPAR- γ in patients with gastric adenocarcinoma. *Exp Oncol* 2016; 38: 191-194.
11. He XW, Yu X, Liu T, Yu SY, Chen DJ. Vector-based RNA interference against vascular endothelial growth factor-C inhibits tumor lymphangiogenesis and growth of colorectal cancer in vivo in mice. *Chin Med J (Engl)* 2008; 121: 439-444.
12. Zhang FL, Gao EY, Shu RB, Wang H, Zhang Y, Sun P, Li M, Tang W, Jiang BQ, Chen SQ, Cui FB. Human recombinant endostatin combined with cisplatin based doublets in treating patients with advanced NSCLC and evaluation by CT perfusion imaging. *Asian Pac J Cancer Prev* 2015; 16: 6765-6768.
13. Ni Q, Ji H, Zhao Z, Fan X, Xu C. Endostar, a modified endostatin inhibits non-small cell lung cancer cell in vitro invasion through osteopontin-related mechanism. *Eur J Pharmacol* 2009; 614: 1-6.
14. Jain RK. Normalization of tumor vasculature: an emerging concept in antiangiogenic therapy. *Science* 2005; 307: 58-62.
15. Ciarrocchi A, Piana S, Valcavi R, Gardini G, Casali B. Inhibitor of DNA binding-1 induces mesenchymal features and promotes invasiveness in thyroid tumour cells. *Eur J Cancer* 2011; 47: 934-945.
16. Hasegawa J, Sue M, Yamato M, Ichikawa J, Ishida S. Novel anti-EPHA2 antibody, DS-8895a for cancer treatment. *Cancer Biol Ther* 2016; 17: 1158-1167.
17. Mahlberg R, Lorenzen S, Thuss-Patience P, Heinemann V, Pfeiffer P, Mohler M. New perspectives in the treatment of advanced gastric cancer: S-1 as a novel oral 5-FU therapy in combination with cisplatin. *Chemotherapy* 2016; 62: 62-70.
18. Hayashi N, Kataoka H, Yano S, Kikuchi JI, Tanaka M, Nishie H, Kinoshita Y, Hatano M, Nomoto A, Ogawa A, Inoue M, Mizoshita T, Shimura T, Mori Y, Kubota E, Tanida S, Joh T. Anticancer effects of a new aminosugar-conjugated platinum complex agent against cisplatin-resistant gastric cancer. *Anticancer Res* 2016; 36: 6005-6009.
19. Fiteni F, Paget-Bailly S, Messenger M, NGuyen T, Lakkis Z, Mathieu P, Lamfichekh N, Picard A, Benzidane B, Cleau D, Bonnetain F, Borg C, Mariette C, Kim S. Docetaxel, Cisplatin, and 5-Fluorouracil as perioperative chemotherapy compared with surgery alone for resectable gastroesophageal adenocarcinoma. *Cancer Med* 2016; 5: 3085-3093.
20. Ma CH, Jiang R, Li JD, Wang B, Sun LW, Lv Y. Experimental study of Endostar injection concomitant with cryoablation on lung adenocarcinoma A549 xenografts. *Asian Pac J Cancer Prev* 2013; 14: 6697-6701.
21. Kaluri R, Reddy CP. A framework for sign gesture recognition using improved genetic algorithm and adaptive filter. *Cog Eng* 2016; 3: 1251730.
22. Kaluri R, Ch P. Sign gesture recognition using modified region growing algorithm and adaptive genetic fuzzy classifier. *Int J Intell Eng Syst* 2016; 9: 225-233.
23. Jain CR, Kaluri R. Design of automation scripts execution application for selenium webdriver and test NG framework. *ARNP J Eng Appl Sci* 2015; 10: 2.
24. Kaluri R, Reddy CHP. An enhanced framework for sign gesture recognition using hidden markov model and

- adaptive histogram technique. *Int J Intell Eng Syst* 2017; 10: 11-19.
25. Kaluri R, Lakshmana K, Reddy T, Karnam S, Koppu S. A comparative study on selecting and ranking the test cases in software testing. *ARN J Eng Appl Sci* 2016; 11: 754-757.

Department of General Surgery
School of Medicine
Shandong University
PR China

***Correspondence to**

Hongzhi Sun